

Turbulent Enhancement of Particle and Heat Fluxes during Sawtooth Oscillations in a Tokamak Edge Plasma

T. L. Rhodes,^(a) Ch. P. Ritz, and H. Lin

Fusion Research Center, The University of Texas, Austin, Texas 78712

(Received 11 January 1990)

Using Langmuir probes in the edge plasma of the TEXT tokamak we have identified sawtooth oscillations in density, potential, and temperature. Concurrent with the sawtooth oscillations are increases in the density and potential fluctuation levels which result in significant increases in the fluctuation-driven particle flux and associated heat flux. No changes in the basic turbulence mechanism were observed during the sawtooth passage.

PACS numbers: 52.55.Fa, 52.35.Kt, 52.35.Mw

The phenomenon of sawtooth oscillations was identified early in the history of tokamak research¹ and was first seen as sawtooth-shaped modulations of the soft-x-ray signal from the interior regions of the tokamak. In that first work the oscillations were identified as due to a periodic loss of energy confinement resulting in a heat pulse propagating from hotter to colder regions of the plasma. Sawtooth-induced oscillations have subsequently been identified in the electron density²⁻⁴ and, most recently, the plasma potential.⁵

Because of the locally perturbing nature of the sawtooth-induced heat and density pulses they have been used to probe the electron thermal diffusivity^{6,7} χ_e and diffusion coefficient D_e .³ The values of χ_e obtained are from 2 to 10 times those derived from other methods, indicating that the heat pulse propagates much faster through the plasma than expected from the energy confinement times.⁷ Fredrickson *et al.*⁷ suggested that either an anomalously high value of χ_e , due perhaps to fluctuations, or an inward heat pinch could explain the differences in the χ_e obtained. Hossain *et al.*⁸ found that the different values of χ_e could be explained on the basis of coupled heat flow and plasma diffusion, but they could not rule out enhanced transport due to magnetic or electrostatic fluctuations. If turbulent transport is driven by temperature or density gradients (as predicted by many theories), the passage of a heat or density pulse would cause the resulting transport coefficients to be significantly different from their equilibrium values.⁹ Namely, the passage of the sawtooth would increase the local plasma parameters (e.g., n_e , \tilde{n}_e , etc.), increasing the turbulence-driven heat and particle fluxes and resulting in the heat and particle pulses propagating out much faster than expected in the unperturbed case. It is known that a major part of the particle and heat transport in the edge plasma is due to fluctuation-driven transport^{10,11} and so it is important to study the turbulent transport during the sawtooth passage.

Periodic enhancements of the high-frequency density fluctuation levels have been observed on several tokamaks.^{2,12,13} The enhancements appear in the fre-

quency range 50–2000 kHz and occur near the sawtooth peak, either just before or just after the sawtooth crash. However, to date, no information has been obtained on the turbulent transport levels themselves.

In this paper we report results from Langmuir probes on the TEXT tokamak with which we measured the effect of sawtooth oscillations on the edge density, temperature, and potential as well as the first measurement of their effect on the fluctuation-driven particle and heat fluxes. The Langmuir probes are constructed of 2-mm-long, 0.5-mm-diam molybdenum wires and were located on a radially movable drive at the top midline of the torus, separated $\sim 160^\circ$ toroidally from the poloidal limiter. Standard three-probe techniques¹⁴ were used to measure the local densities, temperatures, and potentials. The TEXT tokamak¹⁵ itself is a medium-sized Ohmically heated tokamak with a major radius $R_0=1.0$ m, circular minor radius $a=0.26$ m, and full poloidal titanium-carbide-coated carbon-tile limiter.

Figure 1 shows a time history of the chord-averaged soft-x-ray signal from a chord whose tangent radius was $r/a \approx 0.53$ and where the sawtooth inversion radius was

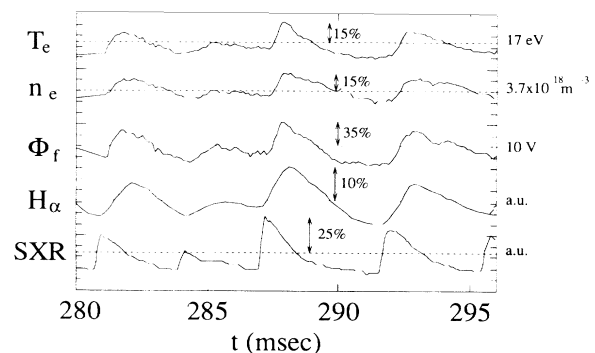


FIG. 1. Time traces of soft-x-ray signal, central chord H_α , and T_e , n_e , and ϕ_f from probes located at $r_{\text{probe}}/a=1.06$. Average values (dotted lines) are shown along with the percentage deviation about the average. $B_\phi=22$ kG, $I_p=325$ kA, $q_a \approx 2.3$, and $\tilde{n}_e=4.5 \times 10^{19} \text{ m}^{-3}$.

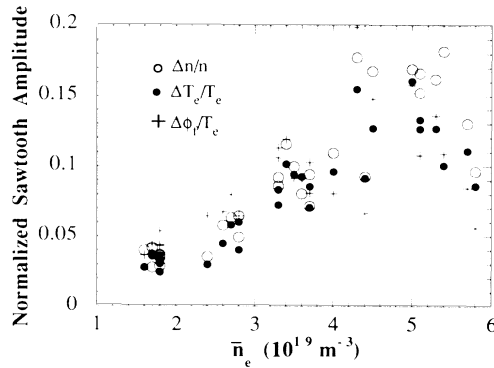


FIG. 2. Normalized sawtooth amplitudes of edge n_e , T_e , and ϕ_f . $B_\Phi = 22$ kG, $I_p = 325$ kA, $q_a \approx 2.3$, and $r_{\text{probe}}/a = 1.06$.

$r/a \approx 0.47$. The plasma conditions for this discharge were 22 kG, 325 kA, and $4.5 \times 10^{19} \text{ m}^{-3}$ with the safety factor at the limiter $q_a \approx 2.3$. Plotted in the same figure are local electron density n_e , electron temperature T_e , and floating potential ϕ_f from the Langmuir probes and H_α from a central viewing chord located at the limiter. All signals show the typical sawtooth behavior of a fast rise followed by a slow decay repeating with a period τ of ~ 4 msec. Also note the smaller than average sawtooth at ~ 284 msec. At this plasma condition the edge parameters n_e and T_e are modulated by approximately 15%. For these data, the probes were located at $r/a = 1.06$; similar results were seen for all positions attainable by the Langmuir probes (generally $r/a \geq 0.95$ on TEXT). The largest sawteeth were seen at low values of the safety factor q_a where the inversion radius is the farthest out.

The normalized sawtooth amplitudes $\Delta n_{\text{st}}/n$, $\Delta T_{e,\text{st}}/T_e$, and $\Delta \phi_{f,\text{st}}/T_e$ (T_e and n_e are the mean values, and Δn_{st} , $\Delta T_{e,\text{st}}$, and $\Delta \phi_f$ are the respective sawtooth amplitudes) of the edge sawtooth modulations were approximately equal in magnitude and increased with increasing \bar{n}_e (Fig. 2). There were indications of a saturation in these normalized amplitudes for $\bar{n}_e \geq 5 \times 10^{19} \text{ m}^{-3}$. This is currently under investigation. The sawtooth perturbation can be a significant fraction of the local density or temperature, varying from 4% to 18% depending on the chord-averaged density. Consistent with these observations, the amplitude of the central soft-x-ray sawteeth also increased as \bar{n}_e increased.

We examine next the effect of the sawtooth passage on the density and floating-potential fluctuation levels, \tilde{n}_e and $\tilde{\phi}_f$, in the edge plasma. Figure 3(a) shows time traces of \tilde{n}_e and $\tilde{\phi}_f$, averaged over multiple sawtooth cycles and plotted as a function of time normalized to the sawtooth period τ_{st} . Here $\tilde{n}_e = \langle (n_e - \langle n_e \rangle)^2 \rangle^{1/2}$, where the time average $\langle \dots \rangle$ was over 0.7 msec (approximately 15% of the sawtooth period τ_{st}) and the data were sampled at 1 MHz, giving 700 points per time average (similarly for the floating-potential fluctuation $\tilde{\phi}_f$).

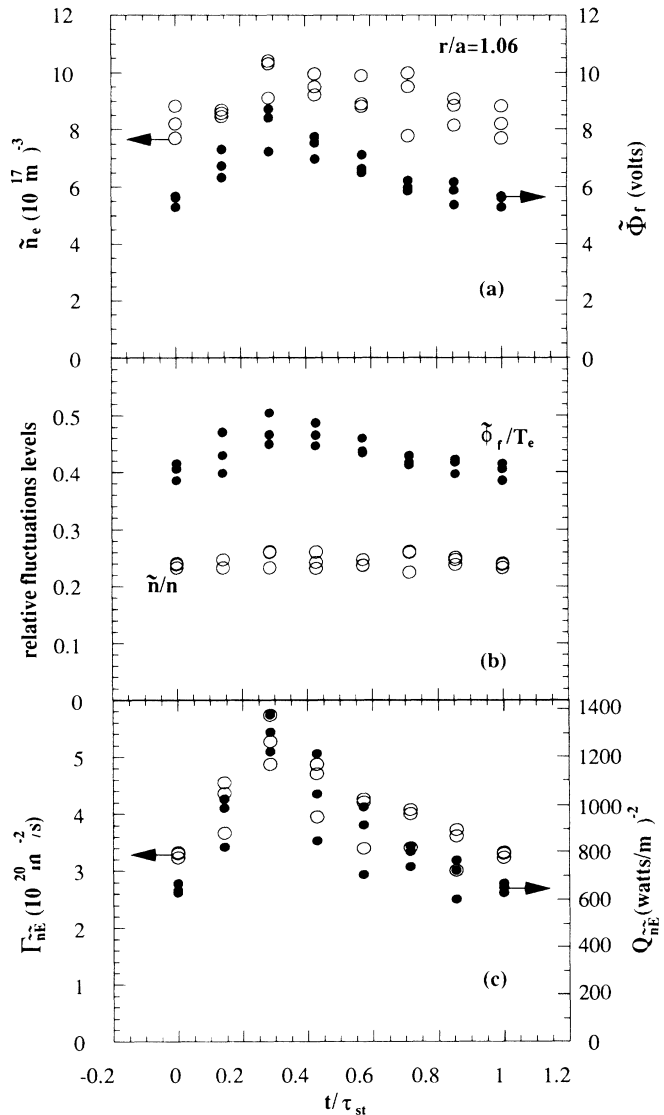


FIG. 3. (a) \tilde{n}_e and $\tilde{\phi}_f$, (b) \tilde{n}_e/n_e and $\tilde{\phi}_f/T_e$, and (c) $\Gamma_{\tilde{n}_e}$ and $Q_{\tilde{n}_e}$ vs t/τ_{st} (sawtooth period $\tau_{\text{st}} \sim 4.0$ msec). Peak of local density and temperature sawtooth (not shown) occurs at $t/\tau_{\text{st}} \approx 0.3$. $B_\Phi = 22$ kG, $I_p = 325$ kA, $q_a \approx 2.3$, $\bar{n}_e = 5.4 \times 10^{19} \text{ m}^{-3}$, and $r_{\text{probe}}/a = 1.06$.

Three macroscopically similar discharges are plotted, producing the three points at each value of t/τ_{st} . The points at $t/\tau_{\text{st}} = 0$ are repeated at $t/\tau_{\text{st}} = 1$. For these plasma parameters the peak values of \tilde{n}_e and $\tilde{\phi}_f$ are 20% and 45% larger than their respective minima. The modulations of \tilde{n}_e and $\tilde{\phi}_f$ have the characteristic sawtooth shape and are in phase with the local n_e and T_e sawteeth (the peaks of the local n_e and T_e sawteeth occur at $t/\tau_{\text{st}} \approx 0.3$). In general, the percentage increases due to the sawteeth were generally larger for $\tilde{\phi}_f$ than for \tilde{n}_e .

The relative fluctuation levels \tilde{n}_e/n_e and $\tilde{\phi}_f/T_e$ remained unequal during the sawtooth passage [Fig.

3(b)], and both they and the poloidal wave number scaled as they would during a parameter scan.^{16,17} Also, the density-potential phase relationship remained unaltered ($\sim\pi/2$ rad).¹⁸ Thus, we found no evidence of changes in the basic turbulent mechanism during the sawtooth.

As previously mentioned, the edge heat and particle transport can be explained on the basis of fluctuation-driven transport.^{10,11} A major part of this transport is due the correlation between fluctuations in the density \tilde{n}_e and radial velocity \tilde{v}_r . Here we assume \tilde{v}_r is due to a fluctuating electric field $\tilde{v}_r = (\tilde{\mathbf{E}} \times \mathbf{B}_\phi) \cdot \hat{\mathbf{r}} / B_\phi^2$ (B_ϕ is the toroidal magnetic field). The fluctuation-driven particle flux $\Gamma_{\tilde{n}_\phi}$ and associated heat flux $Q_{\tilde{n}_\phi}$ are given by $\Gamma_{\tilde{n}_\phi} = \langle n_e(t) E_\theta(t) \rangle / B_\phi$ and $Q_{\tilde{n}_\phi} = \frac{3}{2} T_e \Gamma_{\tilde{n}_\phi}$. Here T_e is in electron volts and the poloidal electric field E_θ is found using $E_\theta = -\Delta\phi_f / \Delta x$, where $\Delta\phi_f = \phi_{f,1} - \phi_{f,2}$ is the difference in the floating potential between two poloidally separated probes and Δx is the poloidal probe separation.

The poloidal electric field E_θ , fluctuating at the sawtooth frequency, was found to be approximately zero, making the low-frequency contribution to $\Gamma_{\tilde{n}_\phi}$ and $Q_{\tilde{n}_\phi}$ zero. Thus, there was no enhancement of the flux $\Gamma_{\tilde{n}_\phi}$ from fluctuations at the sawtooth frequency (that is, at the dominant low-frequency component of the sawtooth oscillation). However, there was significant enhancement of $\Gamma_{\tilde{n}_\phi}$ at higher frequencies (10–250 kHz) due to the increased density and potential fluctuation levels. This is seen in Fig. 3(c) which shows $\Gamma_{\tilde{n}_\phi}$ vs t/τ_{st} and where we have used the same averaging technique as in Figs. 3(a) and 3(b). The magnitude of $\Gamma_{\tilde{n}_\phi}$ increases by approximately 60% from the sawtooth minimum to the sawtooth maximum. The maximum in the particle flux, like the maxima in the fluctuation levels \tilde{n}_e and $\tilde{\phi}_f$, occurs at the peak of the local temperature and density sawteeth. Figure 3(c) also shows the heat flux $Q_{\tilde{n}_\phi}$ vs t/τ_{st} . During the sawtooth cycle the heat flux is increased by approximately 100% over its minimum value and these increases are likewise in phase with the local n_e and T_e sawteeth. The sawtooth modulations of $\Gamma_{\tilde{n}_\phi}$ and $Q_{\tilde{n}_\phi}$ were observed to increase as \tilde{n}_e increased up to $\tilde{n}_e \approx 5 \times 10^{19} \text{ m}^{-3}$, where indications of a saturation occurred. The variation of the related particle confinement time τ_p is, however, a more complicated function of \tilde{n}_e . As \tilde{n}_e increases, the total number of particles N_{tot} in the tokamak dominates in the particle confinement time $\tau_p = N_{tot} / \int \Gamma dA$. Saturation in τ_p occurs^{16,17} when increases in $\Gamma_{\tilde{n}_\phi}$ with \tilde{n}_e become equal to increases in N_{tot} . The percentage modulation of $\Gamma_{\tilde{n}_\phi}$ and $Q_{\tilde{n}_\phi}$ by the sawtooth (a maximum of 60% and 100%, respectively) is much larger than the percentage modulation of the local n_e and T_e (15%–20%). This is a distinct enhancement of the particle and heat fluxes, in phase with the sawtooth cycle, which could be interpreted by other diagnostics (soft x ray, interferometer, etc.) as diffusive and which

would significantly alter the calculation of the local steady-state D_e and χ_e . The role of \tilde{T}_e and related heat flux $Q_{\tilde{T}_e} = 3n\langle \tilde{T}_e \tilde{E}_\theta \rangle / 2B_\phi$ is currently being investigated.

We also examined the effect of the sawtooth on the local density, temperature, and potential gradients. By simultaneously recording n_e , ϕ_f , and T_e from two radial positions (radial separation 0.5 cm, same toroidal position) we could make a two-point estimate of the gradients during the sawtooth cycle. Variations of these gradients at the sawtooth period were unresolved within the ambient turbulence levels and so we concluded that the gradient changes, due to the sawtooth, were 10% or less. Using a 24-channel far-infrared interferometer, Kim *et al.*³ examined the density pulse associated with the sawtooth. From their published data we infer that the maximum scale length of the density perturbation (due to the sawtooth) at the edge is approximately 5 to 6 cm. A radial probe separation of 0.5 cm would then observe an approximately 8%–10% difference in the sawtooth amplitude. Our observation of a gradient change of less than 10% is then consistent with these earlier observations.

We can define coefficients D_{eff} and χ_{eff} by $D_{\text{eff}} = \Gamma_{\tilde{n}_\phi} / |\nabla_r n_e|$ and $\chi_{\text{eff}} = 3Q_{\tilde{n}_\phi} / 2n |\nabla_r T_e|$ which have the same dimensions as transport coefficients. However, we must be careful if we want to interpret them as transport coefficients without knowing the driving terms for the turbulence. In the far-edge plasma the fluxes are predominantly due to electrostatic turbulence which is not necessarily driven by density or temperature gradients.¹⁷ Taking the gradients as constant over the sawtooth period, we found that the mean values for D_{eff} and χ_{eff} were approximately 3.5 and 4.8 m^2/sec , respectively, for the conditions shown in Fig. 3. As the gradients $\nabla_r n_e$ and $\nabla_r T_e$ were modulated less than 10% by the sawtooth oscillation, the defined coefficients D_{eff} and χ_{eff} were modulated by an amount similar to that seen in $\Gamma_{\tilde{n}_\phi}$ (10%–60%). Since \tilde{n}_e/n_e was approximately constant during the sawtooth, the modulation of D_{eff} can be attributed to the modulation of $\tilde{\phi}_f$. However, the modulation in χ_{eff} is due to a combination of T_e and $\tilde{\phi}_f$ both being modulated by the sawtooth.

In comparing the edge and interior observations we find the following: (1) Sawteeth in both density and temperature have been observed in the interior regions of a tokamak.³ These density and temperature sawteeth are observed to be in phase with each other.¹⁹ We have observed similar sawteeth in the far edge which are also in phase. This indicates that, although the dominant transport mechanism may differ in different regions of the plasma, the relative strengths of the transport mechanisms (between the heat and particle fluxes) remain the same as the sawtooth travels outward. (2) Enhanced density fluctuation levels, associated with sawteeth, have been observed both in the interior^{2,12} and now in the edge plasmas. In the edge plasma, this, along with the

increased potential fluctuation levels, results in increased heat and particle fluxes during the sawtooth. (3) On TEXT, the thermal diffusivities from heat-pulse propagation studies χ_{hp} and power balance χ_{pb} disagree by a factor of from 2 to 3,²⁰ while other tokamaks see a factor of from 2 to 10.^{6,7} Various authors have explained these differences as due to an enhanced heat flux during the sawtooth passage.^{2,7,15} At the edge, we have observed just such enhanced heat and particle fluxes during the passage of the sawtooth, consistent with this hypothesis.

We have measured the effects of the sawtooth oscillations only in the far edge and scrape-off layer of the TEXT tokamak $0.95 \leq r/a \leq 1.15$. The inference that fluctuations or fluxes also change with sawtooth oscillations in the deep interior of the plasma should not be made without further experimental work. However, if similar turbulent enhancements to the fluxes occurred in the deep bulk plasma, the heat-pulse method of determining χ_e would necessarily include their effect. This is because it includes all heat fluxes that modify the local heat pulse. It would then give a larger value of χ_e because of the inclusion of transport due to nonconductive means. The enhanced fluctuation levels occur at the peak of the T_e sawtooth mimicking a ∇T_e or diffusive behavior, indistinguishable from a purely diffusive mechanism.⁷ The power-balance and heat-pulse methods would then give different values of χ_e .

In conclusion, significant sawtooth oscillations in local n_e , ϕ_f , and T_e have been observed in the far edge $0.95 \leq r/a \leq 1.15$ of the TEXT tokamak. Associated with these oscillations are increases in the fluctuations \tilde{n}_e and $\tilde{\phi}_f$ which result in an increased fluctuation-driven particle flux $\Gamma_{\tilde{n}\tilde{\phi}}$ and heat flux $Q_{\tilde{n}\tilde{\phi}}$. As the electrostatic fluctuations dominate the particle and heat fluxes in the edge,¹¹ the particle and heat fluxes are coupled resulting in a coupled modulation of the density and temperature during the sawtooth passage. The sawtooth modulations of the fluxes significantly modify the local transport levels (as much as 60% and 100% of $\Gamma_{\tilde{n}\tilde{\phi}}$ and $Q_{\tilde{n}\tilde{\phi}}$, respectively). Further, the modulations of the edge parameters (n_e , T_e , \tilde{n}_e , $\tilde{\phi}_f$, $\Gamma_{\tilde{n}\tilde{\phi}}$, and $Q_{\tilde{n}\tilde{\phi}}$) were in phase with one another. The amplitudes of the modulations of all these edge quantities were found to increase with increasing \tilde{n}_e and decreasing q_a , with indications of an amplitude saturation for $\tilde{n}_e \geq 5 \times 10^{19} \text{ m}^{-3}$. As discussed earlier, the variation of confinement times was a more complicated function of \tilde{n}_e . Although there were enhanced fluctuation levels during the sawtooth, we found no evidence for changes in the basic turbulence mechanism during the sawtooth passage. We presented evidence that all the characteristics of the sawtooth seen in the plasma interior were observed in the edge plasma. Therefore, the conclusions drawn from the edge sawtooth behavior could be relevant for the plasma interior as well and could explain

the discrepancy between the heat-pulse and power-balance determinations of the electron thermal diffusivity χ_e .

We would like to acknowledge helpful and stimulating discussions with Roger D. Bengtson, A. J. Wootton, D. L. Brower, and K. W. Gentle. Brackin A. Smith is thanked for the information on the soft x rays. The construction of the probes, probe drive, and electronics is due to K. C. Carter and his work is gratefully acknowledged. We would also like to thank the entire TEXT team for their efforts. This work was supported by the U.S. Department of Energy, Office of Fusion Energy, under Grant No. DE-FG05-88ER-53267.

^(a)Present address: Institute of Plasma and Fusion Research, Electrical Engineering Department, University of California, Los Angeles, CA 90024.

¹S. von Goeler, W. Stodiek, and N. Sauthoff, *Phys. Rev. Lett.* **33**, 1201 (1974).

²A. Rogister *et al.*, *Nucl. Fusion* **26**, 797 (1986).

³S. K. Kim, D. L. Brower, W. A. Peebles, and N. C. Luhman, Jr., *Phys. Rev. Lett.* **60**, 577 (1988).

⁴A. Komori *et al.*, *Nucl. Fusion* **28**, 1460 (1988).

⁵P. M. Schoch *et al.*, in *Proceedings of the Sixteenth European Conference on Controlled Fusion and Plasma Physics, Venezia, Italy, March 1989* (European Physical Society, Petit-Lancy, Switzerland, 1989), p. 967.

⁶J. D. Callen and G. L. Jahns, *Phys. Rev. Lett.* **38**, 491 (1977).

⁷E. D. Fredrickson *et al.*, *Nucl. Fusion* **26**, 849 (1986).

⁸M. Hossain *et al.*, *Phys. Rev. Lett.* **58**, 487 (1987).

⁹K. W. Gentle, *Phys. Fluids* **31**, 1105 (1988).

¹⁰W. L. Rowan *et al.*, *Nucl. Fusion* **27**, 1105 (1987).

¹¹Ch. P. Ritz *et al.*, *Phys. Rev. Lett.* **62**, 1844 (1989).

¹²D. Brower *et al.*, in *Proceedings of the Fourteenth European Conference on Controlled Fusion and Plasma Physics, Madrid, Spain, June 1987*, edited by F. Engelmann and J. L. Alvarez Rivas, *Europysics Conference Abstracts* (European Physical Society, Petit-Lancy, Switzerland, 1987), p. 1314.

¹³J. Andreoletti *et al.*, *Plasma Phys. Controlled Fusion* **31**, 643 (1989).

¹⁴Sin-Li Chen and T. Sekiguchi, *J. Appl. Phys.* **36**, 2363 (1965).

¹⁵K. W. Gentle, *Nucl. Technol. Fusion* **1**, 479 (1982).

¹⁶W. L. Rowan, C. C. Klepper, Ch. P. Ritz, R. D. Bengtson, K. W. Gentle, P. E. Phillips, T. L. Rhodes, B. Richards, and A. J. Wootton, *Nucl. Fusion* **27**, 1105 (1987).

¹⁷T. L. Rhodes, Ph.D. dissertation, The University of Texas at Austin, 1989 (unpublished).

¹⁸Ch. P. Ritz, Roger D. Bengtson, S. J. Levinson, and E. J. Powers, *Phys. Fluids* **27**, 2956 (1984).

¹⁹D. L. Brower *et al.*, *Phys. Rev. Lett.* **65**, 337 (1990).

²⁰A. J. Wootton *et al.*, in *Proceedings of the Eleventh International Conference on Plasma Physics and Controlled Nuclear Fusion Research, Kyoto, Japan, 1986*, edited by J. W. Weil and M. Demir (IAEA, Vienna, 1987), Vol. 1, p. 187.